IET Control Theory & Applications

Brief Paper

IET Journals
The Institution of Engineering and Technology

Geometric-based PID control design with selective harmonic mitigation for DC–DC converters by imposing a norm bound on the sensitivity function

ISSN 1751-8644
Received on 29th June 2020
Revised 29th October 2020
Accepted on 18th November 2020
E-First on 27th January 2021
doi: 10.1049/iet-cta.2020.0768
www.ietdl.org

Rafael F.Q. Magossi[1,2] ✉, Sangjin Han[3], Ricardo Q. Machado[2], Vilma A. Oliveira[2], Shankar P. Bhattacharyya[3]

[1]*Federal Center for Technological Education, CEFET/RJ, Nova Friburgo, Rio de Janeiro, Brazil*
[2]*Department of Electrical and Computing Engineering, Universidade de Sao Paulo, Sao Carlos, SP, Brazil*
[3]*Department of Electrical and Computer Engineering, Texas A&M University, College Station, TX, USA*
✉ *E-mail: rafael.magossi@cefet-rj.br*

Abstract: The DC–DC converters usually interfaces renewable energy sources in DC microgrids which may be contaminated by harmonic perturbations that adversely affect performance, creates stability and protection problems in a DC grid system. In this paper, the authors propose the use of the popular proportional–integral–derivative (PID) controller to mitigate selected harmonics. The solution is obtained by computing the complete set of stabilising controllers and imposing a bound on the sensitivity function. Using matrix representation of conic sections, the geometric-based PID controller is derived in the controller parameter space. The main result finds a subset of the stabilising set in which the controller mitigate harmonics with prescribed levels of attenuation which are constructively determined for each frequency of the selected harmonics. Simulation and experimental results using a boost converter are provided for validation.

1 Introduction

The growing interest in DC microgrids and DC nanogrids is a natural consequence of the encouraging use of renewable energy sources (RES) as most of them already generates DC power [1]. The DC–DC converters play a central role in DC microgrids since they are generally used to ensure the maximum power extraction as well as to guarantee appropriate levels of voltage/current from power supply to the DC grid [2, 3]. Due to the intermittency of RES, the variations of voltage/current may produce fluctuating DC voltage, which creates stability and protection problems in the DC grid [4]. In this context, the controllers used in the DC–DC converters may significantly contribute to solving the problem of DC voltage fluctuations.

The fixed order proportional–integral (PI) and/or proportional–integral–derivative (PID) controllers are widely used in many industrial applications [5] and have been used as the main control technique in DC–DC converters [6]. While many tuning methods and theories are rigorously established to deliver good stability margins and step reference tracking performance, it is still not thoroughly investigated how to tune the controller gains to provide good disturbance attenuation.

In power electronics applications, the amplitude of selected harmonics needs to be attenuated, if not rejected, to attain voltage distortion limits [7, 8]. Disturbance rejection of the selected harmonics can be guaranteed by requiring a resonant term for each harmonic frequency in the denominator of the controller [9, 10]. However, such a resonant term increases the controller order by two and high order controllers in practice are not always desirable due to their fragility [5]. The disturbance rejection problem for DC–DC converters have also been solved using predictive controllers [11, 12], observer-based integral sliding mode [13], fuzzy strategy [14] and optimised active disturbance rejection control [15].

In [16], the selective harmonic current control was an appealing solution since each selected harmonic was separately detected and controlled in its own reference frame. In [17], a fast selective harmonic current mitigation strategy was presented for inverters with active power filter capabilities based on synchronous reference frames. However, the controllers used in [16] or [17] usually increases the closed-loop system order as much as the number of harmonics.

On the other hand, current analytical design of PID controllers offers the possibility to consider the stabilising set and performance constraints at the same time. As a matter of fact, in [18], a method to tune PI controllers achieving prescribed gain and phase margins was developed. The method used the stabilising set of PI controllers given in [5, 19]. Nonetheless, the selective harmonic mitigation considering the widely used PID controller has not been addressed yet.

A class of methods focuses on the specification of bounds for the sensitivity function. For instance, in [20], PI controllers were parameterised in terms of gain and phase margins, $\mathscr{H}_\infty$ norm bounds on the error transfer function and frequency response of plant transfer function and the stability is analysed by checking the boundary region of the allowed PI gains. An overview of PID controller tuning methods based on specifications on the infinity-norm of the sensitivity functions can be found in [21]. More recently, in [22], the system maximum sensitivity was related do the gain and phase margins and it was tailored by using an exponential error weight in the commonly used square-of-error functions, that is, the ISE and ITSE criteria. The sensitivity analysis was also considered with a fractional-order PID controller in [23].

Applications using PID and specifications of bounds were also considered in the literature. For instance, in [24], the authors consider the problem of optimisation of the mixed sensitivity applied to a buck converter. However, it was a conservative solution in which the proposed method considered all frequencies even though only a few frequencies are required to be taken into account [7].

In this paper, we use the stabilising set for PID controllers [5, 19] and results to synthesise a PI/PID controller with an $\mathscr{H}_\infty$ norm [25] to design a PI/PID controller which tracks step reference signals and mitigates selective harmonics disturbances present in DC microgrids systems. Preliminary results for a PI controller with a single disturbance signal were presented in [26] and summarised

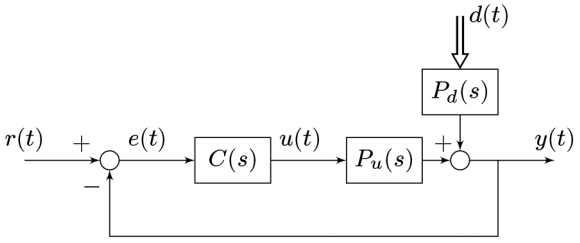

Fig. 1 *Unity feedback system under disturbance*

in [27]. In this paper, we extended the results of [26] for a PID case with multiple disturbance signals by using matrix representation of conic sections to describe the upper bound on the sensibility function and considered a DC–DC converter application which was validated by simulation and experimental results.

The paper is organised as follows. Section 2, following this introduction, summarises the design constraint approach of [25] and in Section 3, a design procedure of PI/PID controllers is proposed. In Section 4, a numerical example is presented in order to illustrate the construction of the stabilising sets along with performance specifications. Also, in Section 4, experimental results are presented to illustrate the application of the proposed method in mitigating harmonics present in an input voltage source. Finally, some concluding remarks are presented in Section 5.

2 Preliminaries

Let $P_u(s)$ and $P_{\rm d}(s)$ be the controlled and disturbance plants, respectively, then consider the unity feedback control loop with disturbance $d(t)$ as shown in Fig. 1. It is assumed that $r(t), u(t), y(t), e(t) \in \mathbb{R}$ and $d(t) \in \mathbb{R}^q$.

The system sensitivity function is defined as

$$S_u(s) =: \frac{1}{1 + P_u(s)C(s)}. \tag{1}$$

Accordingly with [25], given a bound $\gamma > 0$ for the $\mathscr{H}_\infty$ norm on the sensitivity function, we can write

$$\left\| \frac{1}{1 + P_u(s)C(s)} \right\|_\infty < \gamma \tag{2}$$

which is equivalent to

$$\left| 1 + P_u(j\omega)C(j\omega) \right| > \frac{1}{\gamma}, \quad \forall\, \omega \in [0, \infty). \tag{3}$$

Condition (3) implies that the magnitude of the sensitivity function has to be $< \gamma$ for all frequency in the range $[0, \infty)$. In the next section, we apply bounds on some selected frequencies rather than the entire interval $[0, \infty)$.

3 Main results

Using the internal model principle, we can find a sufficient condition for a stabilising controller to track the reference $r(t)$ and reject a class of disturbance signals. Denote the reference and disturbance signals in the Laplace domain as

$$R(s) := \frac{n_{\rm r}(s)}{d_{\rm r}(s)}, \quad D(s) := \left[\frac{n_{d_1}(s)}{d_{d_1}(s)} \quad \cdots \quad \frac{n_{d_q}(s)}{d_{d_q}(s)} \right]^{\rm T} \tag{4}$$

and let

$$P_u(s) = \frac{n_{P_u}(s)}{d_{P_u}(s)}, \quad C(s) = \frac{n_C(s)}{d_C(s)},$$

$$P_{\rm d}(s) = \left[P_{d_1}(s) \quad \cdots \quad P_{d_q}(s) \right] := \left[\frac{n_{P_{d_1}}(s)}{d_{P_{d_1}}(s)} \quad \cdots \quad \frac{n_{P_{d_q}}(s)}{d_{P_{d_q}}(s)} \right].$$

where $n_{P_u}(s), d_{P_u}(s), n_C(s), d_C(s), n_{\rm r}(s), d_{\rm r}(s), n_{d_i}(s), d_{d_i}(s)$ for $i = 1, \ldots, q$ are polynomials in s.

Considering that $d_{P_u}(s) = d_{P_{d_1}}(s) = \cdots = d_{P_{d_q}}(s)$, in this case the error transfer function can be expressed as

$$E(s) = \frac{d_{P_u}(s)d_C(s)}{d_{\rm cl}(s)} \frac{n_{\rm r}(s)}{d_{\rm r}(s)} - \sum_{i=1}^{q} \frac{d_C(s)n_{P_{d_i}}(s)}{d_{\rm cl}(s)} \frac{n_{d_i}(s)}{d_{d_i}(s)} \tag{5}$$

where the closed-loop characteristic polynomial is

$$d_{\rm cl}(s) = d_C(s)d_{P_u}(s) + n_C(s)n_{P_u}(s). \tag{6}$$

The disturbed system output is

$$y(t) = y_{\rm r}(t) + \sum_{i=1}^{q} y_{di}(t) \tag{7}$$

where $y_{\rm r}(t)$ and $y_{di}(t)$ are the output components due to reference and disturbance signal $d_i(t)$, respectively. Suppose that each disturbance signal $d_i(t)$ has a fundamental frequency f_i and it is composed by the sum of sinusoidal signals, called *harmonics*, as

$$d_i(t) = \sum_{h=1}^{m_i} A_{h_{d_i}} \sin(\omega_{h_{d_i}} t) \tag{8}$$

where $A_{h_{d_i}} \in \mathbb{R}$ is called the harmonic amplitude and $\omega_{h_{d_i}} =: 2\pi h f_i \in \mathbb{R}^+$ the harmonic frequency. Then,

$$\begin{aligned} D_i(s) &= \mathscr{L}^{-1}\left\{ \sum_{h=1}^{m_i} A_{h_{d_i}} \sin(\omega_{h_{d_i}} t) \right\} \\ &= \sum_{h=1}^{m_i} \frac{A_{h_{d_i}} \omega_{h_{d_i}}}{s^2 + \omega_{h_{d_i}}^2} \end{aligned} \tag{9}$$

such that $D(s) = \left[D_1(s) \quad D_2(s) \quad \cdots \quad D_q(s) \right]^{\rm T}$.

If $d_{\rm cl}(s)$ is Hurwitz, the steady state error $e(t)$ due to reference input and disturbance goes to zero if and only if the controller $C(s)$ is designed such that $d_{\rm r}(s)$ divides $d_C(s)$ and $d_{d_i}(s)$ divides $d_C(s)$ for $i = 1, \ldots, q$ and $d_{d_i}(s)$ divides $d_C(s)$ for $i = 1, \ldots, q$.

However, to completely reject the harmonics at the output, resonant terms as in (9) are needed. On the other hand, we consider the use of the popular PID controller to solve the problem of mitigation in power electronics by constraining the output at given selective harmonics to acceptable levels. Our goal is thus to propose a PID design method in order to bound the magnitude response due to disturbances, that is, bound the disturbance output

$$y_{\rm d}(t) = \sum_{i=1}^{q} y_{di}(t). \tag{10}$$

Let $Y_{\rm d}(s)$ and $Y_{d_i}(s)$ be the Laplace's transform of $y_{\rm d}(t)$ and $y_{di}(t)$, respectively. Then, from Fig. 1 by superposition, we can write

$$Y_{\rm d}(s) = {\rm S}_u(s)P_{\rm d}(s)D(s) \tag{11}$$

$$= \sum_{i=1}^{q} {\rm S}_u(s)P_{d_i}(s)D_i(s) = \sum_{i=1}^{q} Y_{d_i}(s) \tag{12}$$

and

$$\left| Y_{\rm d}(s) \right| = \left| \sum_{i=1}^{q} Y_{d_i}(s) \right| \le \sum_{i=1}^{q} \left| Y_{d_i}(s) \right|. \tag{13}$$

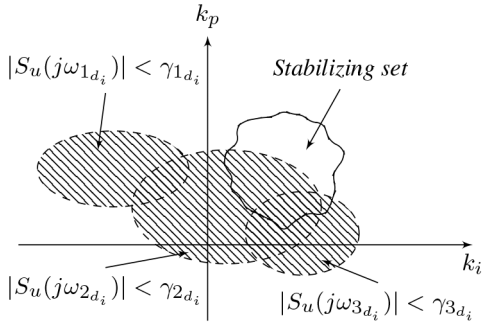

Fig. 2 *Parametric PI controller plane. The gains in the stabilising set which lies outside of the ellipses satisfy the harmonic mitigation condition*

Let $\tilde{\gamma}_{h_{d_i}}$ be a prescribed upper bound for the amplitude of output $y(t)$ relative to the corresponding harmonic h_{d_i} in the steady-state. That is, assuring

$$| Y_{d_i}(s) | < \tilde{\gamma}_{h_{d_i}}$$

which implies that from (8), as the disturbance signals are sinusoidal signals, we can bound the frequency response magnitude using

$$| \mathrm{S}_u(j\omega_{h_{d_i}}) | < \frac{\tilde{\gamma}_{h_{d_i}}}{\left|P_{d_i}(j\omega_{h_{d_i}})\right|\left|A_{h_{d_i}}\right|} =: \gamma_{h_{d_i}} \tag{14}$$

or

$$\left|1 + P_u(j\omega_{h_{d_i}})C(j\omega_{h_{d_i}})\right| > \frac{1}{\gamma_{h_{d_i}}} \tag{15}$$

Note that, (15) has the same form of (3) and thus we can design a controller to mitigate each harmonic present in the disturbance signal by prescribing the magnitude of the frequency response of the sensitivity function at $\omega_{h_{d_i}}$. To ensure closed-loop stability, we obtain the stabilising PID gains in the parameter space using the signature method from [5, 19] by solving a linear inequality system.

Next, we design PI/PID controllers that render a stable closed-loop satisfying (15) by using the matrix representation of conic sections.

3.1 Geometric-based PID controller design

The classical PID controller is given by

$$C(s) = \frac{k_\mathrm{d}s^2 + k_\mathrm{p}s + k_\mathrm{i}}{s(\tau s + 1)}. \tag{16}$$

Assumption 1: The plant has no $j\omega$ axis zeros located at $\omega_{h_{d_i}}$, which yields

$$| P_u(j\omega_{h_{d_i}}) | \neq 0. \tag{17}$$

Now, write

$$P_u(j\omega_{h_{d_i}}) = \phi + j\theta, \quad C(j\omega_{h_{d_i}}) = C_1 + jC_2$$

with

$$C_1 = \frac{\tau k_\mathrm{d}\,\omega_{h_{d_i}}^2 + k_\mathrm{p} - \tau k_\mathrm{i}}{\tau^2\omega_{h_{d_i}}^2 + 1}, \quad C_2 = -\frac{k_\mathrm{i} - k_\mathrm{d}\,\omega_{h_{d_i}}^2 + \tau k_\mathrm{p}\,\omega_{h_{d_i}}^2}{\omega_{h_{d_i}}\left(\tau^2\omega_{h_{d_i}}^2 + 1\right)}.$$

Then, define $| \Psi |$ as the reciprocal of $| \mathrm{S}_u(j\omega_{h_{d_i}}) |$ in (14) and write

$$| \Psi | = | 1 + (\phi + j\theta)(C_1 + jC_2) | > \frac{1}{\gamma_{h_{d_i}}} \tag{18}$$

or

$$\Re(\Psi)^2 + \Im(\Psi)^2 > \frac{1}{\gamma_{h_{d_i}}^2} \tag{19}$$

which for a fixed τ and k_d results in the following conic section

$$\alpha_1 k_\mathrm{i}^2 + \alpha_2 k_\mathrm{i} + \alpha_3 k_\mathrm{p}^2 + \alpha_4 k_\mathrm{p} + \alpha_5 > 0 \tag{20}$$

where

$$\begin{aligned}
\alpha_1 &= \theta^2 + \phi^2 \\
\alpha_2 &= 2\omega_{h_{d_i}}\left(\theta - \phi\,\tau\,\omega_{h_{d_i}}\right) - 2\,k_\mathrm{d}\,\omega_{h_{d_i}}^2\alpha_1 \\
\alpha_3 &= \omega_{h_{d_i}}^2\alpha_1 \\
\alpha_4 &= 2\omega_{h_{d_i}}^2\left(\phi + \theta\,\tau\,\omega_{h_{d_i}}\right) \\
\alpha_5 &= \alpha_1\omega_{h_{d_i}}^4 k_\mathrm{d}{}^2 - \left(2\,\theta - 2\,\phi\,\tau\,\omega_{h_{d_i}}\right)\omega_{h_{d_i}}^3 k_\mathrm{d} \\
&\quad + \omega_{h_{d_i}}^2 + \tau^2\,\omega_{h_{d_i}}^4 - \frac{\omega_{h_{d_i}}^2\left(\tau^2\,\omega_{h_{d_i}}^2 + 1\right)}{\gamma_{h_{d_i}}^2}
\end{aligned}$$

Let $x := \begin{bmatrix} k_\mathrm{i} & k_\mathrm{p} & 1 \end{bmatrix}^\mathrm{T}$ be the homogeneous coordinate vector, then we can obtain the matrix representation of the conic section (20) as

$$H_1(k_\mathrm{i}, k_\mathrm{p}) := x^\mathrm{T}\mathscr{A}x > 0 \tag{21}$$

such that

$$\mathscr{A} = \begin{bmatrix} \alpha_1 & 0 & \frac{\alpha_2}{2} \\ \bullet & \alpha_3 & \frac{\alpha_4}{2} \\ \bullet & \bullet & \alpha_5 \end{bmatrix}$$

with $\bullet$ being the transposed element. Using this matrix representation is can be shown that the conic section is a non-degenerate ellipse, since the leading principal minor of order 2 is

$$\alpha_1\alpha_3 = \omega_{h_{d_i}}^2(\theta^2 + \phi^2)^2 > 0, \quad \forall\theta, \phi, \omega_{h_{d_i}} \in \mathbb{R}_{>0}.$$

Moreover, the centre of the ellipse (k_{i_c}, k_{p_c}) can be obtained as the solution of

$$\nabla H(k_\mathrm{i}, k_\mathrm{p}) = \left[\frac{\partial H(k_\mathrm{i}, k_\mathrm{p})}{\partial k_\mathrm{i}}, \quad \frac{\partial H(k_\mathrm{i}, k_\mathrm{p})}{\partial k_\mathrm{p}}\right] = [0, \quad 0] \tag{22}$$

which results in

$$\begin{bmatrix} k_{i_c} \\ k_{p_c} \end{bmatrix} = \begin{bmatrix} \alpha_1 & 0 \\ 0 & \alpha_3 \end{bmatrix}^{-1}\begin{bmatrix} -\frac{\alpha_2}{2} \\ -\frac{\alpha_4}{2} \end{bmatrix} = \begin{bmatrix} -\frac{\alpha_2}{2\alpha_1} \\ -\frac{\alpha_4}{2\alpha_3} \end{bmatrix}.$$

Therefore, the controller gains in the stabilising PID parameter space outside of all the ellipses satisfy the sensitivity constraints which we call the harmonic constraint ellipses. The graphical illustration of the developed method in the $k_\mathrm{p} - k_\mathrm{i}$ plane is shown in Fig. 2.

In the next section, we derive the PI controller which guarantees disturbance mitigation under a specified level by prescribing a bound on the sensitivity transfer function.

3.2 Geometric-based PI controller design

The classical PI controller is a special case of the PID controller design presented in Section 3.1 with $\tau = k_d = 0$. The classical PI controller is written as

$$C(s) = k_p + \frac{k_i}{s} \tag{23}$$

Replacing $\tau = k_d = 0$ in (18), we thus obtain the conic section for the PI case denoted as

$$\beta_1 k_i^2 + \beta_2 k_i + \beta_3 k_p^2 + \beta_4 k_p + \beta_5 > 0 \tag{24}$$

where

$$\beta_1 = \theta^2 + \phi^2, \quad \beta_2 = 2\,\theta\,\omega_{h_{d_i}}, \beta_3 = \omega_{h_{d_i}}^2 \beta_1$$

$$\beta_4 = 2\omega_{h_{d_i}}^2 \phi, \quad \beta_5 = \omega_{h_{d_i}}^2 - \frac{\omega_{h_{d_i}}^2}{\gamma_{h_{d_i}}^2}$$

Similarly to the PID case, we can obtain the matrix representation of the conic section (24) as

$$H_2(k_i, k_p) := x^T \mathscr{B} x > 0 \tag{25}$$

such that

$$\mathscr{B} = \begin{bmatrix} \beta_1 & 0 & \frac{\beta_2}{2} \\ \bullet & \beta_3 & \frac{\beta_4}{2} \\ \bullet & \bullet & \beta_5 \end{bmatrix}$$

which is also an ellipse with centre given by

$$\begin{bmatrix} k_{i_c} \\ k_{p_c} \end{bmatrix} = \begin{bmatrix} -\frac{\beta_2}{2\beta_1} \\ -\frac{\beta_4}{2\beta_3} \end{bmatrix}.$$

As in the PID case, the PI controller gains in the stabilising set outside of all the ellipses satisfy harmonic constraint ellipses.

Remark 1: If $\omega_{h_{d_i}} = 0$, then the conic is degenerate and if $\omega_{h_{d_i}} = 1$, then the conic is a circle.

Remark 2: The case where $d_i(t)$ is a constant does not need to be addressed as we know that this disturbance will be completely rejected with PI and PID controllers.

Remark 3: The reference signal $r(t)$ may be a ramp or sinusoidal signal, however, it can not be fully tracked by using a PID controller.

In the next section, we provide examples to illustrate the method developed.

4 Examples

In this section, we present two examples. The first example illustrates the steps of the proposed PID controller design for a theoretical plant and the second, the proposed PI controller design is applied to a DC–DC converter, for which we also present experimental results to show the effectiveness of the proposed method in a practical application.

4.1 PID controller design

In this first example, we present the steps of the theoretical design of a PID to validate the proposed method. Consider the following system

$$P_u(s) = \frac{s^4 + 28\,s^3 + 198\,s^2 - 484\,s - 6655}{s^5 + 31.5s^4 + 346\,s^3 + 1466\,s^2 + 1655\,s + 500},$$

$$P_{d_1}(s) = \frac{4\,s^5 - s^4 + s^3 - 2\,s^2 + s + 5}{s^5 + 31.5s^4 + 346\,s^3 + 1466\,s^2 + 1655\,s + 500},$$

$$d_1(t) = \sin(5t)$$

and the PID controller as

$$C(s) = \frac{k_p s + k_i + k_d s^2}{s(s\tau + 1)}$$

with $\tau = 0.001$. The objective is to track a step reference signal and attenuate the disturbance, such that at steady state the amplitude for $\omega_{1_{d_1}} = 5$ rad/s is <0.4.

First, we need to obtain the stabilising set. The experienced reader may use Routh–Hurwitz criterion resulting in

$$\begin{aligned}
&b_1 > 0\\
&b_2 > 0\\
&b_2 b_3 - b_1 b_4 > 0\\
&b_5 {b_2}^2 - b_3 b_2 b_4 - b_1 b_6 b_2 + b_1 {b_4}^2 > 0\\
&-b_8 {b_1}^2 b_4 + {b_1}^2 {b_6}^2 + b_8 b_1 b_2 b_3 + b_7 b_1 b_2 b_4\\
&-2\,b_1 b_2 b_5 b_6 - b_1 b_3 b_4 b_6 + b_1 {b_4}^2 b_5 - b_7 {b_2}^2 b_3\\
&+ {b_2}^2 {b_5}^2 + b_2 {b_3}^2 b_6 - b_2 b_3 b_4 b_5 > 0\\
&{b_1}^2 b_2 {b_8}^2 - 2\,{b_1}^2 b_4 b_6 b_8 + {b_1}^2 {b_6}^3 - 2\,b_1 {b_2}^2 b_7 b_8\\
&+ b_1 b_2 b_3 b_6 b_8 + 3\,b_1 b_2 b_4 b_6 b_7 - 2\,b_1 b_2 b_5 {b_6}^2\\
&+ b_1 b_3 {b_4}^2 b_8 - b_1 b_3 b_4 {b_6}^2 - b_1 {b_4}^3 b_7 + b_1 {b_4}^2 b_5 b_6 + {b_2}^3 {b_7}^2\\
&+ {b_2}^2 b_3 b_5 b_8 - 2\,{b_2}^2 b_3 b_6 b_7\\
&- {b_2}^2 b_4 b_5 b_7 + {b_2}^2 {b_5}^2 b_6\\
&- b_2 {b_3}^2 b_4 b_8 + b_2 {b_3}^2 {b_6}^2\\
&+ b_2 b_3 {b_4}^2 b_7 - b_2 b_3 b_4 b_5 b_6 > 0\\
&-{b_1}^3 {b_8}^3 + 3\,{b_1}^2 b_2 b_7 {b_8}^2\\
&+{b_1}^2 b_3 b_6 {b_8}^2 + 2\,{b_1}^2 b_4 b_5 {b_8}^2 - 3\,{b_1}^2 b_4 b_6 b_7 b_8 - {b_1}^2 b_5 {b_6}^2 b_8\\
&+{b_1}^2 {b_6}^3 b_7 - 3\,b_1 {b_2}^2 {b_7}^2 b_8 - 3\,b_1 b_2 b_3 b_5 {b_8}^2\\
&+ b_1 b_2 b_3 b_6 b_7 b_8 - b_1 b_2 b_4 b_5 b_7 b_8\\
&+3\,b_1 b_2 b_4 b_6 {b_7}^2 + 2\,b_1 b_2 b_5^2 b_6 b_8 - 2\,b_1 b_2 b_5 {b_6}^2 b_7\\
&- b_1 {b_3}^2 b_4 {b_8}^2 + 2\,b_1 b_3 {b_4}^2 b_7 b_8 + b_1 b_3 b_4 b_5 b_6 b_8\\
&- b_1 b_3 b_4 {b_6}^2 b_7 - b_1 {b_4}^3 {b_7}^2 - b_1 {b_4}^2 {b_5}^2 b_8\\
&+ b_1 {b_4}^2 b_5 b_6 b_7 + {b_2}^3 {b_7}^3 + 3\,{b_2}^2 b_3 b_5 b_7 b_8\\
&-2\,{b_2}^2 b_3 b_6 {b_7}^2 - {b_2}^2 b_4 b_5 {b_7}^2 - {b_2}^2 {b_5}^3 b_8\\
&+ {b_2}^2 {b_5}^2 b_6 b_7 + b_2 {b_3}^3 {b_8}^2 - 2\,b_2 {b_3}^2 b_4 b_7 b_8\\
&- b_2 {b_3}^2 b_5 b_6 b_8 + b_2 {b_3}^2 {b_6}^2 b_7 + b_2 b_3 {b_4}^2 {b_7}^2\\
&+ b_2 b_3 b_4 {b_5}^2 b_8 - b_2 b_3 b_4 b_5 b_6 b_7 > 0\\
&b_8 > 0
\end{aligned}$$

where

$$\begin{bmatrix} b_1 \\ b_2 \\ b_3 \\ b_4 \\ b_5 \\ b_6 \\ b_7 \\ b_8 \end{bmatrix} = \begin{bmatrix} 2\,\tau \\ 63\,\tau + 2\,k_d + 2 \\ 692\,\tau + 56\,k_d + 2\,k_p + 63 \\ 2932\,\tau + 396\,k_d + 2\,k_i + 56\,k_p + 692 \\ 3310\,\tau - 968\,k_d + 56\,k_i + 396\,k_p + 2932 \\ 1000\,\tau - 13310\,k_d + 396\,k_i - 968\,k_p + 3310 \\ 1000 - 13310\,k_p - 968\,k_i \\ -13310\,k_i \end{bmatrix}$$

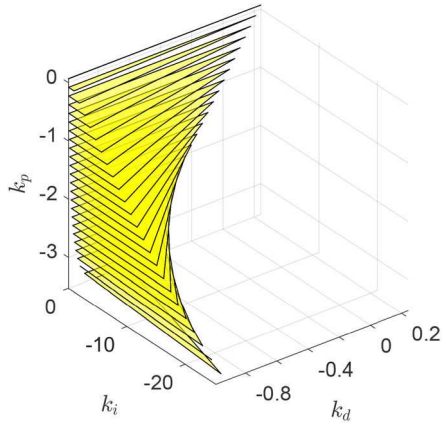

Fig. 3 *PID stabilising set by using the method proposed in [5, 19] formed by linear subsets*

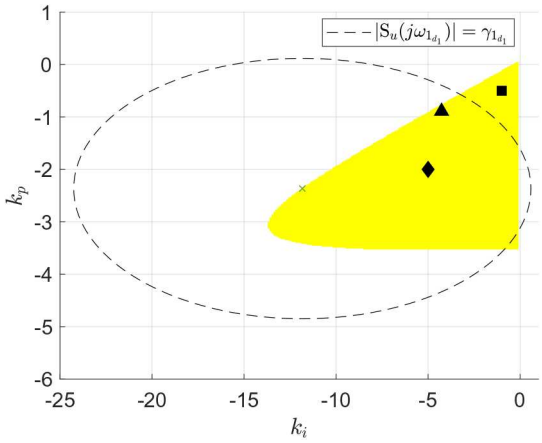

Fig. 4 *Selected PID controller gains in the stabilising set (filled region) of the system with fixed $k_d = -0.8$ and the harmonic constraint ellipse (dashed line). The point 'x' is the centre of the ellipse*

Table 1 Selected PID controller's gains

	Filled square	Filled lozenge	Filled triangle
k_i	−1	−5	−4.27
k_p	−0.5	−2	−0.89

which is highly non-linear inequality system with no straightforward method to solve it. However, using the signature method from [5, 19], the stabilising set can be obtained by fixing k_p gain and solving linear inequality systems. The obtained stabilising set is shown in Fig. 3.

It is desired that $\tilde{\gamma}_{1_{d_1}} = 0.4$. As, $A_{1_{d_1}} = 1$ and $\omega_{1_{d_1}} = 5$ rad/s, we have

$$\left|P_{d_1}(j5)\right| = 0.3457$$

which means that

$$\gamma_{1_{d_1}} = \frac{\tilde{\gamma}_{1_{d_1}}}{\left|P_{d_1}(j5)\right| A_{1_{d_1}}} = 1.1572$$

Following the steps in Section 3.1, we first choose the derivative gain $k_d = -0.8$ from the stabilising set and then we obtain the stabilising subset and the harmonic ellipse on the $k_p - k_i$ plane as shown in Fig. 4. The gains indicated by filled square and filled lozenge in the stabilising set shown in Table 1 were selected

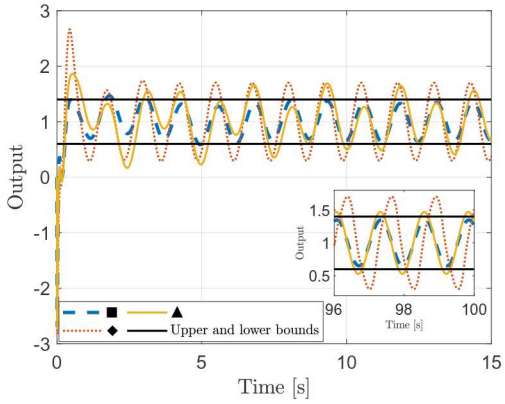

Fig. 5 *Unit step response of the system for the controllers Table 1*

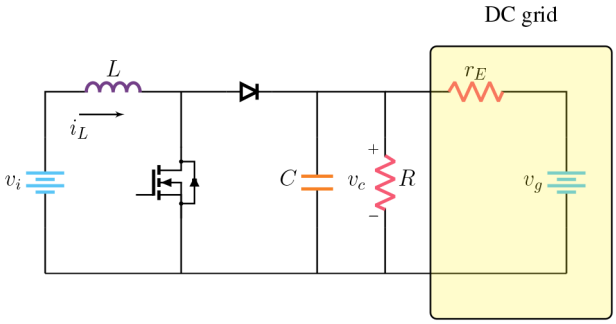

Fig. 6 *Boost DC–DC converter topology used in the simulation results*

to be tested. In order to show the effectiveness of the proposed method, we performed a classic tuning based on the concepts of bandwidth and phase margin [27]. As $\omega_{1_{d_1}} = 5$ rad/s, for a fair comparison, we selected the bandwidth as half of this value and we obtained the controller (filled triangle) of Table 1 with the same phase margin of filled lozenge using the tuning strategy of [18].

For comparison, the outputs for a step response obtained with all the designed controllers are shown in Fig. 5. Note that, the controller (filled triangle) is reasonably acceptable as it provides an output close to the specified bounds. However, it is important to mention that although filled square and filled triangle share the same phase margin, the proposed method of tuning showed to be less conservative than using bandwidth. The proposed design method guarantees that the resulting controller (filled square) effectively mitigates the harmonics of the disturbance. Moreover, differing from the tuning used for controller (filled triangle), in our approach the designer has the flexibility to take a controller outside of the ellipses that also meet other performance criteria.

The next example is a practical application of a PI controller to a DC–DC converter.

4.2 PI controller design for a boost converter

We explore a practical example of a boost DC–DC converter used to connect a power supply v_i to a DC grid and supply a load R at the same time. The circuit is shown in Fig. 6. The power supply and the DC grid are contaminated with harmonics and the goal is to keep the voltage on the load v_c under acceptable limits.

Let k denote a unit pulsed signal with switching frequency f_s and duty cycle K, $y = v_c$ the output and V_g and V_i the average values of v_g and v_i, respectively. Using the small-signal analysis presented in [28], it is possible to obtain the transfer function (see (26)) , with

$$\delta(s) = s^2 + \frac{L r_E + L R}{C L R r_E} s + \frac{R r_E K^2 - 2 R r_E K + R r_E}{C L R r_E}$$

$$P_u(s) = \frac{y(s)}{k(s)} = \frac{\left(-(R V_i + V_i r_E - V_g R + V_g K R)/C R r_E (K-1)^2\right) s + (V_i/C L)}{\delta(s)} \quad (26)$$

Table 2 Boost converter parameters for simulation

Parameter	Value	Parameter	Value
L	100 μH	V_i	250 V
C	4.7 mF	V_g	450 V
R	10 Ω	K	0.50
r_E	0.50 Ω	f_s	20 kHz

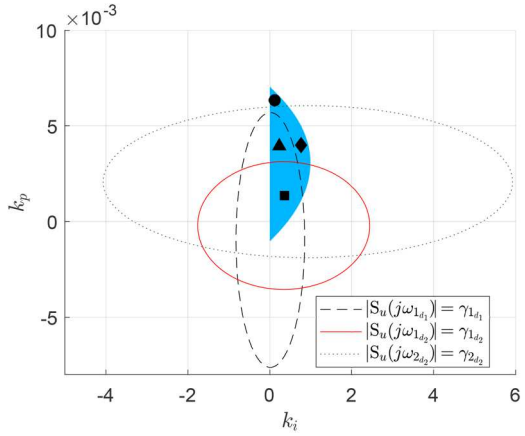

Fig. 7 *Selected PI controller gains in the stabilising set (filled region) of the boost converter system and the harmonic constraint ellipse*

Table 3 Selected PI controller's gains

	Filled square	Filled lozenge	Filled triangle	Filled circle
k_i	0.3606	0.7661	0.2339	0.1325
k_p	0.0014	0.0040	0.0039	0.0063

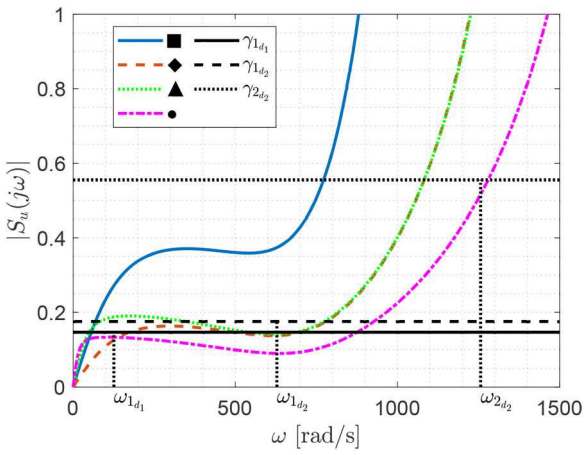

Fig. 8 *Magnitude of the frequency response of $S_u(j\omega)$ of boost converter system for different controllers*

and

$$P_d(s) = \begin{bmatrix} P_{d_1}(s) & P_{d_2}(s) \end{bmatrix} = \begin{bmatrix} \dfrac{y(s)}{v_i(s)} & \dfrac{y(s)}{v_g(s)} \end{bmatrix} \tag{27}$$

$$= \frac{1}{\delta(s)} \begin{bmatrix} -\dfrac{K-1}{C\,L} & \dfrac{1}{C\,r_E}s \end{bmatrix}. \tag{28}$$

Next, the PI controller design is developed.

4.2.1 Controller design: Suppose that in this system the harmonics present in the input voltage, neglecting the DC value, are

$$d_1(t) = \sum_{h=1}^{1} A_{h_{d_1}} \sin(\omega_{h_{d_1}} t) \tag{29}$$

where $A_{1_{d_1}} = 10$, $\omega_{1_{d_1}} = 2\pi 50$ rad/s and the harmonics present in the DC grid voltage, neglecting the DC value, are

$$d_2(t) = \sum_{h=1}^{2} A_{h_{d_2}} \sin(\omega_{h_{d_2}} t) \tag{30}$$

with $A_{1_{d_2}} = 10$, $\omega_{1_{d_2}} = 2\pi 100$ rad/s, $A_{2_{d_2}} = 5$ $\omega_{2_{d_2}} = 2\pi 200$ rad/s.

The design requirements for the controller are to maintain $495 \le v_c \le 505$ and constrain the output harmonic amplitudes to the following upper bounds

$$\tilde{\gamma}_{1_{d_1}} = 3, \quad \tilde{\gamma}_{1_{d_2}} = 0.75, \quad \tilde{\gamma}_{2_{d_2}} = 1.25.$$

Using the boost converter parameters (see Table 2) in (26) and (27), we have

$$P_u(s) = \frac{-6.383 \times 10^4\, s + 5.319 \times 10^8}{s^2 + 446.8\, s + 5.319 \times 10^5}$$

$$P_{d_1}(s) = \frac{1.064 \times 10^6}{s^2 + 446.8\, s + 5.319 \times 10^5}$$

$$P_{d_2}(s) = \frac{425.5 \times s}{s^2 + 446.8\, s + 5.319 \times 10^5}.$$

The PI controller stabilising set is first computed as in [5, 19]. Then, following the steps in Section 3.2, the harmonic constraint ellipses are obtained and it is shown, along with the stabilising set, in Fig. 7. We selected the four points given in Table 3, to show whether the specifications are met or not.

The magnitude of the frequency response of $S_u(j\omega)$ of boost converter system for different controllers is shown in Fig. 8, in which it can be seen that as the point (filled square) lies inside of all ellipses in Fig. 4, thus the controller can not attain the amplitude specification for the harmonics at $\omega_{1_{d_1}}, \omega_{1_{d_2}}$ and $\omega_{2_{d_2}}$. For the point (filled rhombus) in Fig. 4, note that the designed point is inside of the ellipse for $|S_u(j\omega_{2_{d_2}})|$, but outside of $|S_u(j\omega_{1_{d_1}})|$ and $|S_u(j\omega_{1_{d_2}})|$, which means that the controller does only attain the amplitude specification for both $\omega_{1_{d_1}}$ and $\omega_{1_{d_2}}$ as shown in Fig. 8. Related to the point (filled triangle) from Fig. 4, note that the designed point is inside of the ellipse for $|S_u(j\omega_{2_{d_2}})|$ and $|S_u(j\omega_{1_{d_1}})|$, but outside of $|S_u(j\omega_{1_{d_2}})|$, which means that the controller does only attain the amplitude specification for $\omega_{1_{d_2}}$, which is verified in Fig. 8. Finally, for the point (filled circle) in Fig. 4, note that the designed point lies outside of all three ellipses, which means that the controller achieves the amplitude specification for the harmonics at $\omega_{1_{d_1}}$, $\omega_{1_{d_2}}$ and $\omega_{2_{d_2}}$ and as the point filled circle satisfies all the specifications, it was tested on the software PSIM, as shown in Fig. 9.

4.2.2 Experimental results: A particular case of the boost converter shown in Fig. 6 was implemented considering the parameters shown in Tables 4 and 5. In this case, the disturbance were present only in the input voltage and it was described by

$$d(t) = d_1(t) = \hat{v}_{th} = \sum_{h=1}^{1} A_{h_{d_1}} \sin(\omega_{h_{d_1}} t) \tag{31}$$

with $A_{1_{d_1}} = 10$, $\omega_{1_{d_1}} = 2\pi 5$ rad/s. The design requirement for the controller is to keep $115 \le v_c \le 125$ which means $\tilde{\gamma}_{1_{d_1}} = 5$. The input voltage of the boost converter contaminated with a sinusoidal disturbance was implemented via a rapid dSPACE prototyping bench. Thus, a frequency inverter in the voltage source inverter configuration was used with a PI controller and a resonant controller set at the frequency of 5 Hz. The dSPACE bench used and the implemented boost converter are shown in Fig. 10.

The open-loop transition to closed-loop system using a designed controller obtained with the presented method is shown in Fig. 11. The Fourier transform of the experimental boost converter

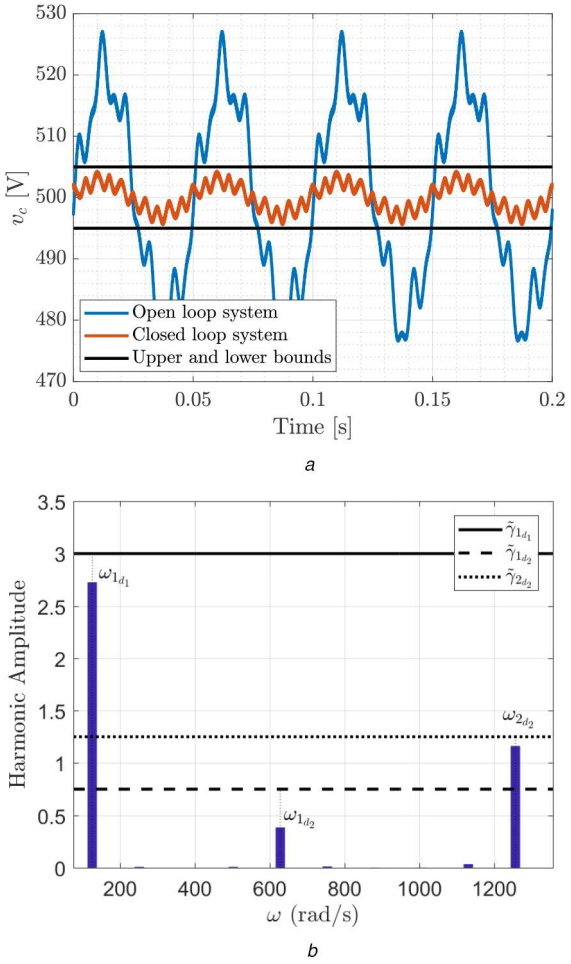

Fig. 9 *Boost converter in PSIM with filled circle controller results*
(a) Boost converter output voltage, ***(b)*** Fourier analysis of the controlled output

Table 4 Boost converter parameters for experimental results

Parameter	Value	Parameter	Value
L	5 mH	V_i	60 V
C	470 μF	V_g	0 V
R	198.31 Ω	K	0.5
r_E	∞ Ω	f_s	20 kHz

output voltage in closed loop is shown in Fig. 12, and it is possible to notice that the 5 Hz harmonic content at the open-loop output is about 15.68 V, which becomes 4.37 V right after the loop closes.

5 Concluding remarks

In this paper, a geometric-based approach for tuning a classical PID controller considering selective harmonic mitigation was presented. In this approach, the stabilising regions in the controller parameter space are used to obtain subsets of the achievable prescribed harmonic level at given frequencies. We showed that by upper bounding the magnitude of the sensitivity transfer function, the subsets in the controller parameter space which mitigate the undesired harmonics lie outside of ellipses in the stabilising regions. With this approach, it was possible to design PID controllers to achieve specifications considering each harmonic present in the system. The physical constraints should then be checked for the selected gains attaining stability and harmonic ellipses. An advantage of the approach is its flexibility to allow the designer to perform a multi-objective design and choose any feasible controller parameters which best meets the design requirements. The presented examples showed the efficiency of the approach to mitigate the harmonics present in the voltage source in

Table 5 Experimental bench devices

Device	Code
diode	DSEI 2X31-06 C
MOSFET	IXFN140N30P
voltage transducer	LEM LV 20-P
current transducer	LEM LA 55-P/SP1
oscilloscope	5054 Digital Phosphor Tektronix
control unit	STM32F429I-DISC1

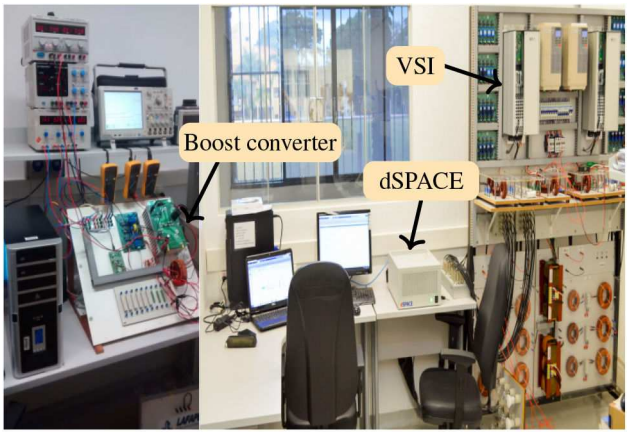

Fig. 10 *Experimental bench with boost converter for selective harmonic mitigation*

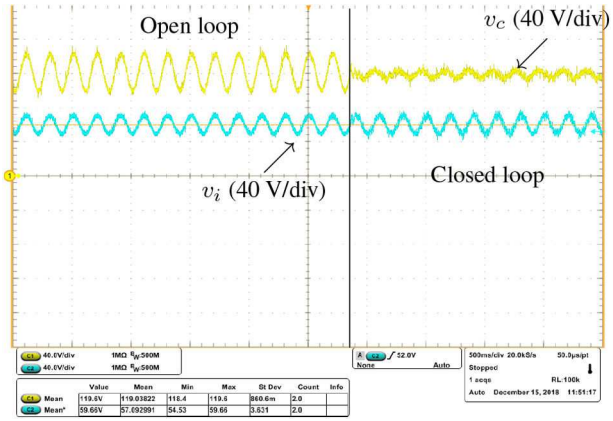

Fig. 11 *Closing the loop around 2.9 s with the designed controller to mitigate the harmonic at the voltage output of the boost converter system. The blue line is the input voltage and the yellow line is the output voltage. The time-scale was 500 ms/div*

DC microgrids applications. Although applied to DC–DC converters, the approach can be used in other practical systems.

6 Acknowledgments

This work received the financial support of the Brazilian National Council for Scientific and Technological Development (CNPq) under grant 305892/2017-7 and the São Paulo Research Foundation (FAPESP) under grants 2016/25017-1, 2016/21120-2, and 2017/21577-5.

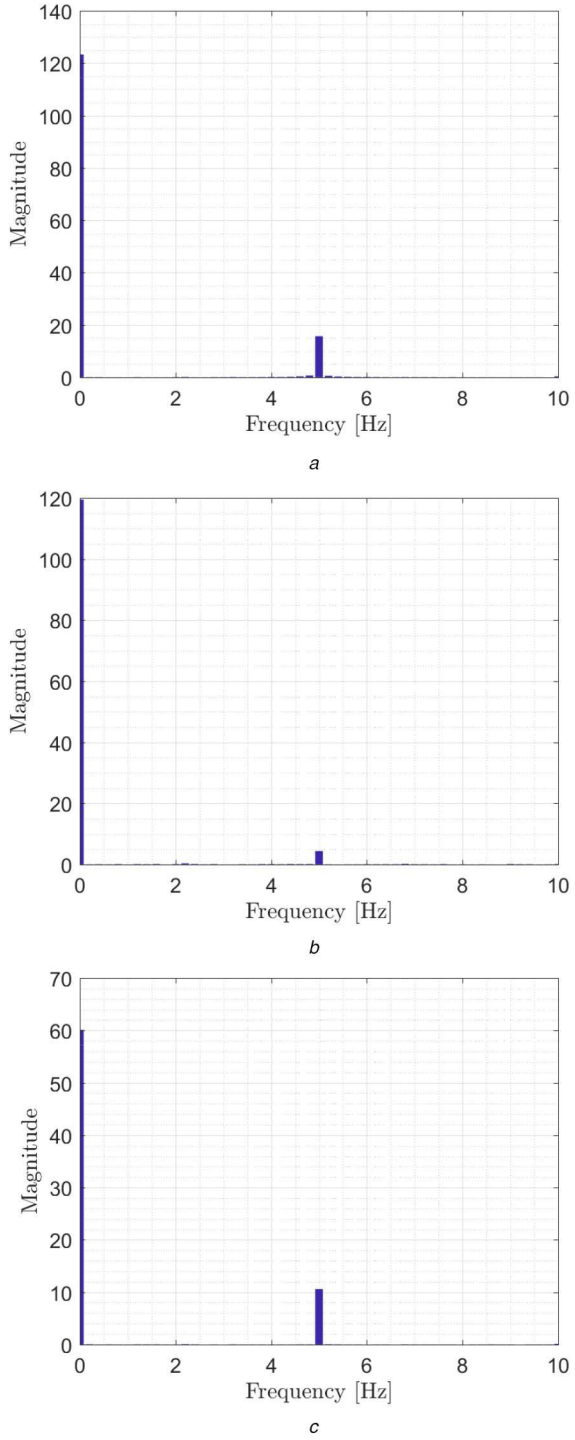

Fig. 12 *Harmonic content of the experimental boost converter input and output voltage. The y-axis is given in volts*

(a) Harmonic content of the output voltage in open loop, ***(b)*** Harmonic content of the output voltage in closed loop, ***(c)*** Harmonic content of the input voltage

7 References

[1] Haroun, R., El Aroudi, A., Cid-Pastor, A., *et al.*: 'Modelling and control of modular DC-nanogrids based on loss-free resistors', *IEEE Access*, 2020, **8**, pp. 33305–33317

[2] Lakshmi, M., Hemamalini, S.: 'Nonisolated high gain DC–DC converter for DC microgrids', *IEEE Trans. Ind. Electron.*, 2018, **65**, (2), pp. 1205–1212

[3] Prabhakaran, P., Agarwal, V.: 'Novel boost-sepic type interleaved DC–DC converter for mitigation of voltage imbalance in a low-voltage bipolar DC microgrid', *IEEE Trans. Ind. Electron.*, 2020, **67**, (8), pp. 6494–6504

[4] Kumar, D., Zare, F., Ghosh, A.: 'DC microgrid technology: system architectures, AC grid interfaces, grounding schemes, power quality, communication networks, applications, and standardizations aspects', *IEEE Access*, 2017, **5**, pp. 12230–12256

[5] Bhattacharyya, S.P., Datta, A., Keel, L.H.: '*Linear control theory: structure, robustness, and optimization*', vol. **33** (CRC press, Boca Raton, FL, USA, 2009)

[6] Fuzato, G.H.F., Aguiar, C.R., Bastos, R.F., *et al.*: 'Evaluation of an interleaved boost converter powered by fuel cells and connected to the grid via voltage source inverter', *IET Power Electron.*, 2018, **11**, (10), pp. 1661–1672

[7] Teodorescu, R., Blaabjerg, F., Borup, U., *et al.*: 'A new control structure for grid-connected LCL PV inverters with zero steady-state error and selective harmonic compensation'. Applied Power Electronics Conf. and Exposition, Anaheim, USA, February 2004, vol. 1, pp. 580–586

[8] Aguiar, C.R., Bastos, R.F., Gonçalves, A.F.Q., *et al.*: 'Frequency fuzzy anti-islanding for grid-connected and islanding operation in distributed generation systems', *IET Power Electron.*, 2015, **8**, (7), pp. 1255–1262

[9] Teodorescu, R., Blaabjerg, F., Liserre, M., *et al.*: 'Proportional-resonant controllers and filters for grid-connected voltage-source converters', *IEE Proc. Electr. Power Appl.*, 2006, **153**, (5), pp. 750–762

[10] Agnoletto, E.J., Castro, D.S., Neves, R.V.A., *et al.*: 'An optimal energy management technique using the ϵ -constraint method for grid-tied and stand-alone battery-based microgrids', *IEEE Access*, 2019, **7**, pp. 165928–165942

[11] Errouissi, R., Al-Durra, A., Muyeen, S.M.: 'A robust continuous-time MPC of a DC–DC boost converter interfaced with a grid-connected photovoltaic system', *IEEE J. Photovolt.*, 2016, **6**, (6), pp. 1619–1629

[12] Shi, Y., Zhou, J., Li, S., *et al.*: 'A combined anti-disturbance strategy of DC-DC converter'. 2017 29th Chinese Control And Decision Conf. (CCDC), Chongqing, China, May 2017, pp. 7384–7388

[13] Pandey, S.K., Patil, S.L., Chaskar, U.M., *et al.*: 'State and disturbance observer-based integral sliding mode controlled boost DC–DC converters', *IEEE Trans. Circuits Syst. II, Exp. Briefs*, 2019, **66**, (9), pp. 1567–1571

[14] Tomescu, B., VanLandinham, H.F.: 'Disturbance rejection and robustness considerations in DC/DC converters'. 30th Annual IEEE Power Electronics Specialists Conf., Charleston, USA, July 1999, vol. 2, pp. 1204–1209

[15] Yang, J., Cui, H., Li, S., *et al.*: 'Optimized active disturbance rejection control for DC-DC buck converters with uncertainties using a reduced-order gpi observer', *IEEE Trans. Circuits Syst. I, Reg. Pap.*, 2018, **65**, (2), pp. 832–841

[16] Lascu, C., Asiminoaei, L., Boldea, I., *et al.*: 'Frequency response analysis of current controllers for selective harmonic compensation in active power filters', *IEEE Trans. Ind. Electron.*, 2009, **56**, (2), pp. 337–347

[17] Campos.Gaona, D., Peña.Alzola, R., Monroy.Morales, J.L., *et al.*: 'Fast selective harmonic mitigation in multifunctional inverters using internal model controllers and synchronous reference frames', *IEEE Trans. Ind. Electron.*, 2017, **64**, (8), pp. 6338–6349

[18] Díaz.Rodríguez, I.D., Bhattacharyya, S.P.: 'PI controller design in the achievable gain-phase margin plane'. IEEE 55th Conf. on Decision and Control, Las Vegas, USA, December 2016, pp. 4919–4924

[19] Ho, M.-T., Datta, A., Bhattacharyya, S.P.: 'A linear programming characterization of all stabilizing PID controllers'. Proc. 1997 American Control Conf., Albuquerque, USA, June 1997, pp. 3922–3928

[20] Yaniv, O., Nagurka, M.: 'Robust PI controller design satisfying sensitivity and uncertainty specifications', *IEEE Trans. Autom. Control*, 2003, **48**, (11), pp. 2069–2072

[21] Doulgeri, Z., Karayiannidis, Y., Garcia, D., *et al.*: 'Robust proportional integral derivative controller tuning with specifications on the infinity-norm of sensitivity functions', *IET Control Theory Appl.*, 2007, **1**, (1), pp. 263–272

[22] Verma, B., Padhy, P.K.: 'Optimal PID controller design with adjustable maximum sensitivity', *IET Control Theory Appl.*, 2018, **12**, (8), pp. 1156–1165

[23] Chen, L., Chen, G., Wu, R., *et al.*: 'Variable coefficient fractional-order PID controller and its application to a sepic device', *IET Control Theory Appl.*, 2020, **14**, (6), pp. 900–908

[24] Omer, P., Kumar, J., Surjan, B.S.: 'Design of robust PID controller for buck converter using bat algorithm'. 2016 IEEE 1st Int. Conf. on Power Electronics, Intelligent Control and Energy Systems, Delhi, India, July 2016, pp. 1–5

[25] Han, S., Keel, L.H., Bhattacharyya, S.P.: 'PID controller design with an $\mathscr{H}_\infty$ criterion'. 3rd IFAC Conf. on Advances in proportional-integral-derivative Control PID, Ghent, Belgium, May 2018, pp. 400–405

[26] Magossi, R.F.Q., Han, S., Oliveira, V.A., *et al.*: 'Proportional-integral controller design for selective harmonic mitigation'. Latin American Conf. on Automatic Control - XVIII CLCA, Quito, Ecuador, October 2018

[27] Díaz.Rodríguez, I.D., Han, S., Bhattacharyya, S.P.: '*Analytical design of PID controllers*' (Springer, Cham, Switzerland, 2019)

[28] Erickson, R.W.: '*Fundamentals of power electronics*' (Chapman & Hall, New York, NY, USA, 1997)